Cell PRESS
Neuron
Article

Ca^{2+}-Dependent Metarhodopsin Inactivation Mediated by Calmodulin and NINAC Myosin III

Che-Hsiung Liu,[1] Akiko K. Satoh,[2,4] Marten Postma,[1,3] Jiehong Huang,[1] Donald F. Ready,[2] and Roger C. Hardie[1,*]
[1]Department of Physiology, Development and Neuroscience, Cambridge University, Cambridge CB2 3DY, UK
[2]Department of Biological Sciences, Purdue University, West Lafayette, IN 47907, USA
[3]Present address: Section Computational Science, Faculty of Science, University of Amsterdam, Kruislaan 403,1098 SJ Amsterdam, The Netherlands
[4]Present address: Division of Biological Sciences, Graduate School of Science, Nagoya University, Furo-cho, Chikusa-ku, Nagoya, Aichi, Japan 466-8601
*Correspondence: rch14@cam.ac.uk
DOI 10.1016/j.neuron.2008.07.007

SUMMARY

Phototransduction in flies is the fastest known G protein-coupled signaling cascade, but how this performance is achieved remains unclear. Here, we investigate the mechanism and role of rhodopsin inactivation. We determined the lifetime of activated rhodopsin (metarhodopsin = M*) in whole-cell recordings from *Drosophila* photoreceptors by measuring the time window within which inactivating M* by photoreisomerization to rhodopsin could suppress responses to prior illumination. M* was inactivated rapidly (τ ~20 ms) under control conditions, but ~10-fold more slowly in Ca^{2+}-free solutions. This pronounced Ca^{2+} dependence of M* inactivation was unaffected by mutations affecting phosphorylation of rhodopsin or arrestin but was abolished in mutants of calmodulin (CaM) or the CaM-binding myosin III, NINAC. This suggests a mechanism whereby Ca^{2+} influx acting via CaM and NINAC accelerates the binding of arrestin to M*. Our results indicate that this strategy promotes quantum efficiency, temporal resolution, and fidelity of visual signaling.

INTRODUCTION

In any signaling cascade, it is important that each step is appropriately terminated in a timely fashion. This is particularly true in phototransduction where rapid response termination is essential for high temporal resolution, and perhaps nowhere more so than in flies, which have the fastest known G protein-coupled signaling cascade (reviews: Montell, 1999; Hardie and Raghu, 2001; Hardie and Postma, 2008; Wang and Montell, 2007). In *Drosophila*, the key elements of this cascade, from rhodopsin to the light-sensitive channels, are localized in a tightly packed array of microvilli forming the light-guiding rhabdomere. Two classes of channels, transient receptor potential (TRP) and TRP-like (TRPL), are activated downstream of phospholipase C (PLC), most likely by lipid products of PLC such as diacylglycerol (DAG), polyunsaturated fatty acids, and/or the reduction in phosphatidyl inositol 4,5 bisphosphate (PIP_2) (reviewed by Minke and Parnas, 2006; Hardie, 2007; Wang and Montell, 2007). The dominant channel is highly Ca^{2+} selective and encoded by the *trp* gene (Montell and Rubin, 1989; Hardie and Minke, 1992). Activation of a single rhodopsin molecule by one photon results in a discrete electrical event, the quantum bump ~10 pA in amplitude, mediated by activation of ~15 TRP channels after a variable latency of ~20–100 ms (Henderson et al., 2000). The associated Ca^{2+} influx transiently raises $[Ca^{2+}]$ to near millimolar levels in the affected microvillus (Postma et al., 1999; Oberwinkler and Stavenga, 2000). This Ca^{2+} influx is critical for response kinetics and amplification, mediating both positive and negative feedback via multiple molecular targets (Hardie, 1991, 1995; Smith et al., 1991; Scott et al., 1997; Gu et al., 2005). However, despite extensive investigation, in most instances the precise mechanisms underlying this feedback are still only poorly understood.

The first stage of excitation is the photoisomerization of rhodopsin (R) to active metarhodopsin (M*) by the *11-cis* to *all-trans* photoisomerization of the chromophore (3-hydroxy-retinal); M* is subsequently inactivated by binding to arrestin (see Figure 8). In vertebrate photoreceptors, M* inactivation is Ca^{2+} dependent because M* must first be phosphorylated by a Ca^{2+} (and recoverin) dependent rhodopsin kinase before arrestin can bind M* (Kawamura, 1993). However, in flies, M* phosphorylation appears not to be required for arrestin binding (Plangger et al., 1994; Vinos et al., 1997; Kiselev et al., 2000; but see Lee et al., 2004), raising the question of whether M* lifetime can be modulated by Ca^{2+} and, if so, how? One possibility was suggested by finding that arrestin itself is rapidly phosphorylated by CaMKII (Matsumoto et al., 1994). However, a subsequent study reported that this was not required for arrestin binding to M but instead was required for arrestin to subsequently dissociate from R *after* M had been photoreisomerized (Alloway and Dolph, 1999), leaving no known mechanism for Ca^{2+}-dependent M* inactivation in *Drosophila*.

Here, we measured M* lifetime by exploiting the bistable nature of invertebrate rhodopsins (Hillman et al., 1983; Stavenga, 1996), whereby M* can be instantaneously inactivated by photoreisomerization to the inactive R state (Hamdorf and Kirschfeld, 1980; Richard and Lisman, 1992). We found that M* inactivation in *Drosophila* is indeed strongly Ca^{2+} dependent. Our results

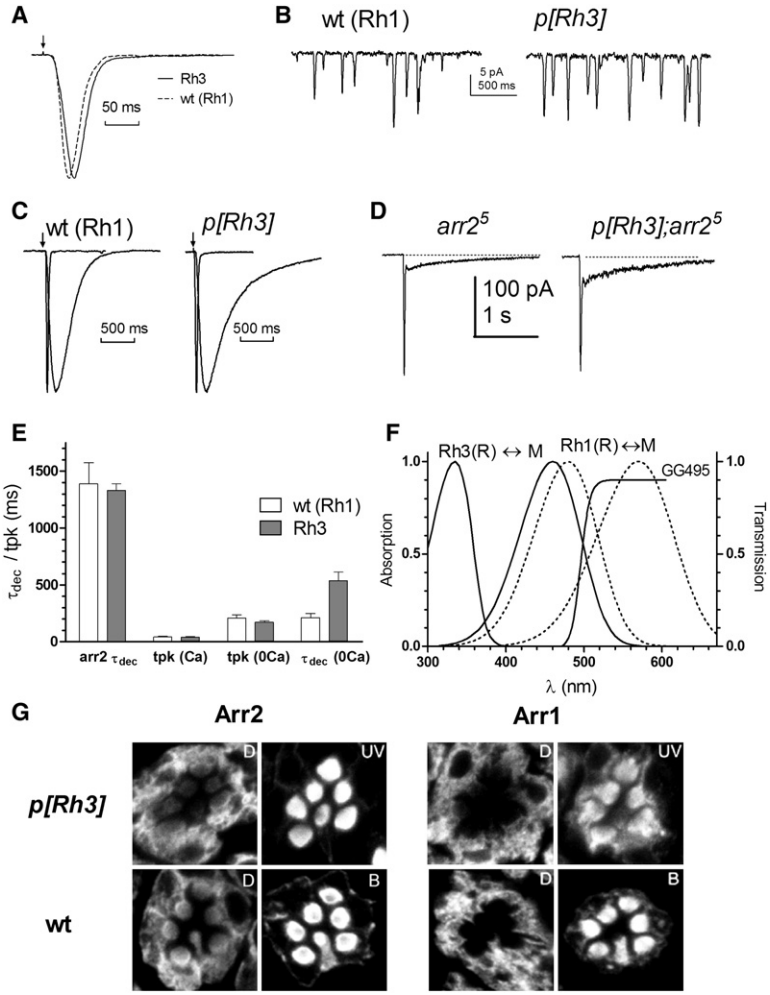

Figure 1. Properties of R1-6 Photoreceptors Expressing Rh3

(A) Averaged, normalized whole-cell voltage-clamped responses to brief (1 ms) flashes (arrows) containing ~100 effective photons in R1-6 photoreceptors of wild-type flies (Rh1) and flies expressing the UV-sensitive Rh3 opsin (*p[Rh3]*).

(B) Quantum bumps elicited by continuous dim illumination.

(C) Normalized responses to brief (1 ms) flashes in the presence (rapid) and absence (slow) of extracellular Ca^{2+}.

(D) Responses to brief flashes in $arr2^5$ null mutant in otherwise wild-type flies (left) and *p[Rh3]* flies (right).

(E) Summary of kinetic parameters: time-to-peak (tpk) in the presence and absence of Ca^{2+}, decay time constant (τ_{dec}) in Ca^{2+}-free solution and also in $arr2^5$ null background (mean ± SD, n = 4–10 cells per data point).

(F) Normalized rhodopsin (R) and metarhodopsin (M) absorption spectra for Rh1 (dotted lines: λ_{max} 470/560 nm) and Rh3 (330/460 nm); spectra based on nomograms (Govardovskii et al., 2000); transmission spectrum of the GG495 filter is also shown.

(G) Immunolocalization of Arr1 and Arr2 in 7-day-old *p[Rh3]* and 0- to 2-day-old wild-type flies; in dark-adapted (D) eyes, Arr2 was distributed both in the cytosol and rhabdomere, while Arr1 was found predominantly in the cytosol. Within 5 min of the appropriate illumination (UV or blue), both had translocated to the rhabdomere: n = 7 flies (wild-type), 2 flies (*p[Rh3]* D), and 5 flies (*p[Rh3]* UV).

further suggest that this is achieved by a mechanism whereby Ca^{2+} influx acting via CaM and myosin III (NINAC) promotes the binding of arrestin to metarhodopsin. This strategy, combined with the ultracompartmentalization afforded by the photoreceptors' microvillar design, promotes quantum efficiency, temporal resolution, and fidelity of visual signaling.

RESULTS

Light Responses Mediated by the UV Opsin Rh3

In order to measure the lifetime of M* in vivo, we used a powerful but rarely used strategy that involves exciting the cell with a test flash and then inactivating M* by photoreisomerization (Hamdorf and Kirschfeld, 1980; Richard and Lisman, 1992). The logic is that photoreconversion of M* should suppress the response to a prior test flash as long as M* is still active, but not if M* has already been inactivated. Critically, the strategy relies on the ability to rapidly reconvert the very same M* molecules that had been initially excited, necessitating the delivery of brief, extremely intense flashes capable of hitting all ~10^8 rhodopsin molecules in the cell. For the case of the major rhodopsin in *Drosophila* (Rh1), the overlap of the M and R absorption spectra makes such an approach impractical, as the reconverting flash itself would also activate sufficient new R molecules to generate a near-saturating response. We therefore used flies (*p[Rh3]*) in which Rh1 had been replaced by the UV-absorbing rhodopsin, Rh3 (Feiler et al., 1992; Ranganathan et al., 1994), where the R and M spectra are sufficiently widely separated that long-wavelength light can reconvert M with minimal excitation of R (Figure 1F).

We first characterized Rh3-mediated responses in order to test whether they resembled responses mediated by Rh1 (Figure 1). In whole-cell voltage-clamped recordings from dissociated ommatidia, responses to brief UV flashes in *p[Rh3]* cells showed similar, albeit slightly slower, kinetics to responses from wild-type photoreceptors; quantum bumps were also similar in waveform, though slightly larger than in wild-type. Importantly for this study, responses showed a similar dependence on Ca^{2+}, with an ~10-fold slowing of both onset and offset kinetics when extracellular Ca^{2+} was removed (Figure 1C), indicating that both positive and negative feedback by Ca^{2+} influx were intact.

Since M* inactivation is believed to be mediated by binding to arrestin (Dolph et al., 1993), it was important to ask whether Rh3 interacts with arrestin in a similar fashion to Rh1. *Drosophila* photoreceptors express two arrestin isoforms: Arr2, which is the dominant isoform required for rapid inactivation of Rh1; and Arr1, which can terminate the response more slowly in the absence of Arr2 (Dolph et al., 1993). A potential complication is that both arrestins translocate to the rhabdomere during illumination (Kiselev et al., 2000; Lee et al., 2003; Satoh and Ready, 2005); in dark-adapted wild-type flies, Arr2 is widely distributed

Table 1. Arrestin Levels in Mutant Backgrounds

	WT	*p[Rh3]*	*ninaC*^{P235}	*ninaC*^{KD}	*cam*	*arr2*^{5}/+
Arr2 level	100%	136%	50% ± 17%	30% ± 16%	28% ± 8%	59% ± 12%
n	18	2	14	5	3	4

Values determined by densitometry of western blots (mean ± SD, normalized to levels in wild-type using tubulin as standard), see Experimental Procedures and Figure S1 for further details.

throughout the cell with only a relatively small (~30%) fraction in the rhabdomere, while Arr1 is almost exclusively localized in the cell body. Immunocytochemistry showed that both Arr2 and Arr1 were similarly distributed in *p[Rh3]* flies and that both translocated reversibly in response to UV illumination (Figure 1G). We also confirmed by western analysis that Arr2 was expressed at wild-type levels in *p[Rh3]* flies (Table 1 and Figure S1 available online).

To confirm functional involvement of Arr2 in inactivation of Rh3, we used a null allele of the *arr2* gene (*arr2*^{5}) and found that responses in *p[Rh3];arr2*^{5} flies showed a deactivation defect very similar to that previously described in *arr2* mutants. Namely, responses initially inactivated normally due to Ca^{2+}-dependent inactivation of the channels but then failed to rapidly reach baseline, leaving a secondary peak or shoulder that decayed over several seconds (Figure 1D). Finally, the phenotypes of several other phototransduction mutants, including *norpA* (PLC), *Gαq*, *ninaC*, and *cam* (calmodulin), were reproduced when investigated on the *p[Rh3]* background (Figure S2 and see below). These results clearly establish that Rh3 interacts with Arr2 and Arr1 in a similar fashion to Rh1 and utilizes the same excitation and inactivation signaling machinery.

Photoreisomerization of M* Suppresses the Light Response

The R and M states of Rh3 absorb maximally at 330 nm and 460 nm, respectively (Figure 1F; Feiler et al., 1992). Using a long-wavelength cut-off filter (Schott GG495), it was possible to reconvert >90% of M to R within the duration of a brief flash (~1 ms) delivered by a high-voltage Xe flash lamp. By itself, this yellow (Y) flash generated a modest response equivalent to ~200 effectively absorbed photons, due to residual absorption by the long-wavelength flank of the R absorption spectrum. When delivered 5 ms prior to a brief (1 ms) UV test flash, the responses summated, generating responses approximately equal to the sum of the responses to Y and UV flashes delivered alone (Figure 2B). However, when the Y flash was delivered 2–5 ms after the UV flash, the response was greatly reduced and was barely larger than the response to the Y flash delivered alone (Figure 2C). This indicated that virtually all of the M molecules generated by the UV flash were reconverted to R by the Y flash before they had had a chance to activate downstream elements of the transduction cascade.

The effective lifetime of active M* was then probed by varying the timing of the Y reconverting flash relative to UV excitation. Y flashes almost completely suppressed the response to the UV flash when delivered within 5 ms, but then their ability to suppress the response decreased exponentially with a time constant of ~20 ms, and flashes delivered more than ~50 ms after the UV flash no longer caused significant suppression of the response. Comparison of suppressed responses with the control response (UV alone) showed that suppression first started ~20 ms after the reconverting flash (Figure 2E). This delay probably represents the persistence of Gq α subunits and PLC molecules already activated by M* prior to the reconverting flash and which

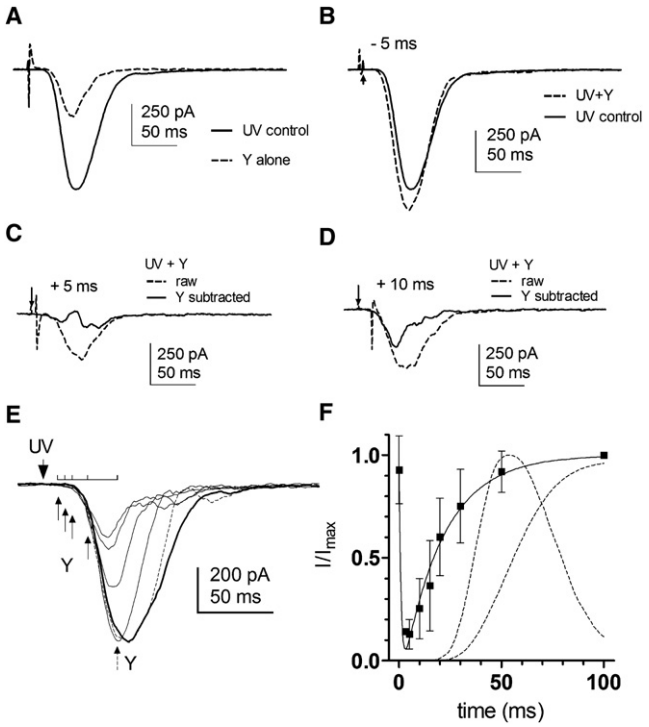

Figure 2. Determination of Active M* Lifetime by M > R Photoreconversion in *p[Rh3]* Flies

(A) Control responses to 1 ms UV flash (solid trace) and reconverting GG495 nm flash (Y) (dotted trace), each delivered alone—the timing of the flashes is indicated by stimulus artifacts.

(B) When the Y flash was delivered 5 ms prior to the UV flash, the responses summated, resulting in a slightly larger response (dotted trace) than to the UV flash alone (solid trace). Timing of UV flash indicated by arrow, Y flash by stimulus artifact.

(C) When the Y flash was delivered 5 ms *after* the UV flash, the overall response (dotted trace) was greatly suppressed; after subtraction of the response to Y alone (solid trace), there was virtually no residual response, showing that the response to UV had been almost entirely suppressed.

(D) When Y was delivered 10 ms after UV, there was a clear but still greatly suppressed residual response.

(E) Residual responses (after subtraction of the Y response template) with increasing Y flash delays (10, 15, 20, 30, and 50 ms). After 50 ms (dotted trace), there was very little remaining suppression compared to the UV control flash (solid thick trace).

(F) Response as a fraction of the control response (I/I_{max} measured from the integral current) as a function of delay of the reconverting flash (mean ± SD, n = 9 cells). Data were fitted with a two-exponential function with 1 ms R > M activation time course (fixed) to derive an effective M* decay time constant of 23 ms. Also shown are the normalized (inverted) control response time course and its cumulative integral (note that the effective M* lifetime appears to be ended by the peak of the response—and approximately follows the cumulative integral with a left time shift of ~35 ms).

are still capable of generating a response. The suppression reflects inactivation (by reconversion to R) of M* molecules, which had not yet activated sufficient G proteins to overcome threshold for bump generation. Following this delay, the suppressed responses inactivated rapidly with a time course τ_{dec} ~7 ms, which is similar to the time course of inactivation of single quantum bumps and is probably mediated by the Ca^{2+}-dependent inactivation of TRP channels.

M* Lifetime Is Ca^{2+} Dependent

These experiments indicate that, under physiological conditions, M* is effectively inactivated with a time constant of ~20 ms. We next asked whether this rapid inactivation depended upon Ca^{2+} influx by repeating the experiments in Ca^{2+}-free solutions where responses are prolonged ~10-fold. Strikingly, reconverting (Y) flashes delivered even at very late times (>500 ms) during such Ca^{2+}-free responses were always capable of suppressing the tail of the response (n = 14), demonstrating that M* had remained active throughout most of the response and was required to sustain the response over these durations (Figure 3). Suppression of such responses by M* reconversion again first started after a short delay of ~25 ms. The response then decayed with a time constant of ~80 ms, providing a direct measurement of the inactivation time course of events downstream of rhodopsin, such as inactivation of the G protein-PLC complex and/or the removal of excitatory messenger (e.g., metabolism of DAG by DAG kinase) under Ca^{2+}-free conditions.

To avoid inaccuracies that might arise from subtraction of the Y flash response template, we also recorded from flies that had been raised on a vitamin A-deprived (VA–) diet that reduced Rh3 concentration ~350-fold. Under these conditions, the Y flash now elicited virtually no response at all by itself, so that suppression by M* reconversion and its kinetics could be directly recorded without needing to subtract a template. Examples shown in Figure 3D directly confirm complete suppression with similar kinetics (τ_{dec} 82 ± 14 ms, n = 7) to that derived after template subtraction in flies reared on normal diet (85 ± 16 ms, n = 8).

These results directly demonstrate that, in the absence of Ca^{2+} influx, M* lifetime is the rate-limiting step controlling response duration and decay. With this knowledge, and since the response under Ca^{2+}-free conditions scales strictly linearly with intensity (R.C.H., unpublished data), the effective lifetime of M* under Ca^{2+}-free conditions can be most conveniently estimated by simply fitting an exponential to the final tail of the flash response. This yielded values of ~500 ms in *p[Rh3]* flies and 200–300 ms (mean 227 ± 44 ms, n = 13) in wild-type photoreceptors (Figure 1E). The dramatic ~10-fold increase in the lifetime of active M* in Ca^{2+}-free solutions indicates that, in the presence of extracellular Ca^{2+}, M* inactivation is rapidly accelerated by the Ca^{2+} influx associated with the quantum bump.

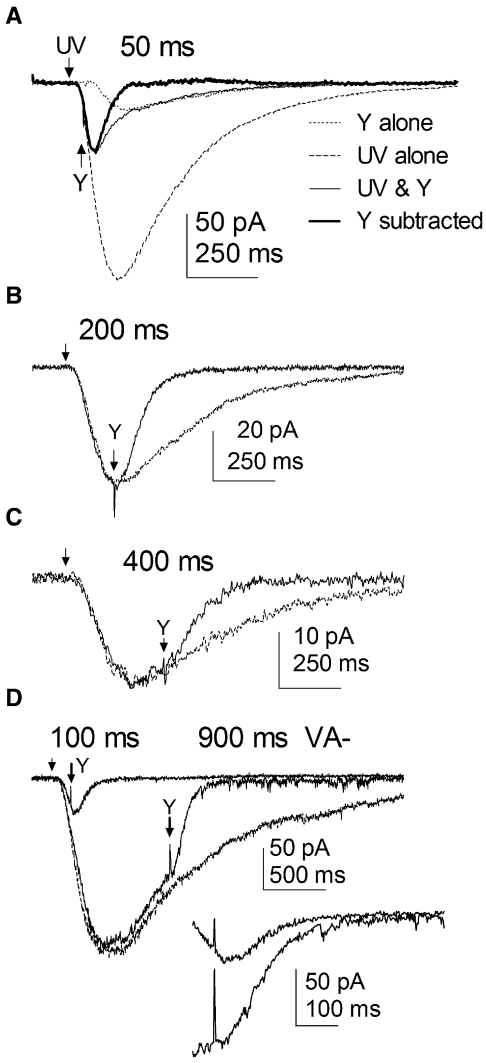

Figure 3. M* Lifetime Is Greatly Prolonged in Ca^{2+}-Free Solutions

(A) Responses from *p[Rh3]* photoreceptor in Ca^{2+}-free solution to UV and Y alone (dotted and stippled traces), superimposed on response to UV and Y delivered together with a 50 ms delay. After subtraction (thick trace), the residual response was greatly suppressed with respect to the UV control and decayed to baseline much faster.

(B and C) After delays of 200 and 400 ms, the Y flash still suppressed the light response (solid trace, after subtraction of response to Y flash alone; dotted traces, control response to UV flash alone). Similar results in n = 7 cells.

(D) Recording from vitamin A-deprived *p[Rh3]* fly (VA–) without template subtraction. The Y flash rapidly suppressed responses when delivered at both 100 and 900 ms after the UV flash (intensity ~500-fold brighter than in [A]–[C]). Inset shows the suppression on a faster timescale after alignment of the two traces; after a delay of ~25 ms, the response decayed to baseline with a time constant of 82 ± 15 ms (n = 7).

Arr2 Overexpression Accelerates Response Termination under Ca^{2+}-Free Conditions

These results demonstrate that M* inactivation is strongly Ca^{2+} dependent in photoreceptors expressing Rh3. The similar Ca^{2+} dependence of Rh1- and Rh3-mediated responses (Figure 1) implies that this is also the case in wild-type photoreceptors; nevertheless, we sought independent confirmation that inactivation of M* by Arr2 is also rate limiting under Ca^{2+}-free conditions for Rh1. If this is the case, then increasing Arr2 levels would be predicted to accelerate response inactivation. To test this, we recorded from *p[Arr2]* flies expressing two extra copies of a wild-type *arr2* transgene, resulting in an approximate doubling of Arr2 protein level (Dolph et al., 1993;

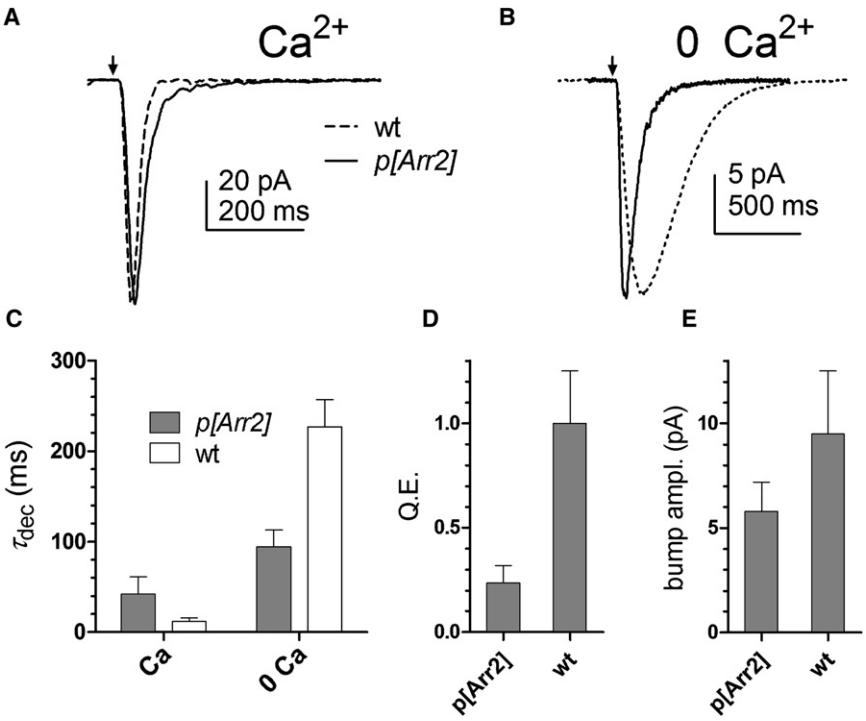

Figure 4. Effects of Overexpression of the Wild-Type *Arr2* Transgene

(A) In the presence of Ca^{2+}, response decay in *p[Arr2]* flies following a brief test flash (1 ms) was significantly slower than in wild-type (dotted trace, responses normalized).

(B) Under Ca^{2+}-free conditions, response deactivation was greatly accelerated in *p[Arr2]* flies, indicating that Arr2 is rate limiting under these conditions.

(C) Time constants of response deactivation (τ_{dec}) in the presence and absence of Ca^{2+} (mean ± SD, n = 11–13 cells).

(D) Quantum efficiency (Q.E.) relative to wild-type was reduced ~5-fold in *p[Arr2]* flies.

(E) Bump amplitude was reduced ~2-fold (mean ± SD, n = 6 cells).

Ranganathan and Stevens, 1995). As predicted, when recorded under Ca^{2+}-free conditions, photoreceptors from *p[Arr2]* flies (four independent transformant lines) showed a greatly accelerated response deactivation, with a decay time constant of 94 ms (Figure 4B). This was not significantly different from the time constant of response inactivation following M > R reconversion under Ca^{2+}-free conditions.

Paradoxically, and contrary to a previous report (Ranganathan and Stevens, 1995), in the presence of physiological Ca^{2+}-containing solutions, responses in *p[Arr2]* flies actually decayed significantly more *slowly* than in wild-type photoreceptors (τ_{dec} ~40 ms, cf. ~12 ms in wild-type), indicating that inactivation of M* by Arr2 is not rate limiting under physiological conditions (Figure 4A). Further analysis revealed that the slow "decay" reflected the generation of quantum bumps with longer latencies (data not shown). In addition, sensitivity to light was substantially reduced due to an ~5 fold reduction in effective quantum efficiency (Q.E.) and an ~2-fold reduction in bump amplitude (Figures 4D and 4E). While initially surprising, these phenotypes can be readily reconciled with current models of quantum bump generation. Thus, bump generation and amplification are thought to involve the sequential and stochastic activation of approximately five or more G proteins and PLC molecules during the bump latent period (Hardie et al., 2002). The reduction in Q.E. in *p[Arr2]* flies is presumably due to the increased levels of Arr2 resulting in a high probability that M* is inactivated before it has a chance to activate a G protein (or sufficient G proteins to initiate a quantum bump). Furthermore, if only one or two G proteins are activated, the reduction in net PLC activity can be expected to result in production of smaller bumps with longer latencies. In these respects, these phenotypes resemble those of hypomorphic G protein mutants (*Gαq*), which also have reduced Q.E. and bump amplitude and prolonged bump latencies (Scott et al., 1995; Hardie et al., 2002).

M* Inactivation Is Ca^{2+} Independent in Arrestin Mutants

Since M* is quenched by binding to the dominant arrestin isoform Arr2 (Dolph et al., 1993), our results imply that inactivation of M* by Arr2 is strongly Ca^{2+} dependent. If this is the case, it may be predicted that the Ca^{2+} dependence of M* termination would be altered or eliminated in *arr2* mutants. We therefore investigated the Ca^{2+} dependence of responses in the null $arr2^5$ mutant. As previously reported (Dolph et al., 1993), responses to brief flashes in $arr2^5$ flies show a prolonged decay lasting several seconds, the tail of which could be fitted with a single exponential of ~1400 ms (Figures 5A and 5E). In confirmation of an earlier study (Scott et al., 1997), the slow deactivation was seen to be due to the ability of single effectively absorbed photons to excite trains of quantum bumps (Figure 5B). This is interpreted as the ability of active M* to reactivate the transduction cascade after a refractory period, probably induced by the massive Ca^{2+} influx in the microvillus that supports the bump (Postma et al., 1999; Oberwinkler and Stavenga, 2000; Mishra et al., 2007). The duration of this refractory period was estimated from the interval distribution between bumps in such trains and peaked at ~100–150 ms, with shortest intervals of ~50 ms (Figure 5B).

Under Ca^{2+}-free conditions, responses in $arr2^5$ were still very significantly (>5-fold) prolonged compared to wild-type responses, with an intermediate time course observed in $arr2^5$/+ heterozygotes (Figures 5C and 5E). This indicates that Arr2 also mediates response termination under Ca^{2+}-free conditions. Significantly, the time course of response decay in $arr2^5$ mutants under Ca^{2+}-free conditions was now indistinguishable from that measured in the presence of Ca^{2+} (Figures 5D and 5E). This indicates that M* inactivation in the absence of Arr2 is Ca^{2+} independent, consistent with the proposal that binding of Arr2 to M* represents the Ca^{2+}-dependent step in M* inactivation. Since M* inactivation in *arr2* null mutants is believed to be mediated by the minor arrestin, Arr1 (Dolph et al., 1993), these results also imply that M* inactivation by Arr1 is Ca^{2+} independent.

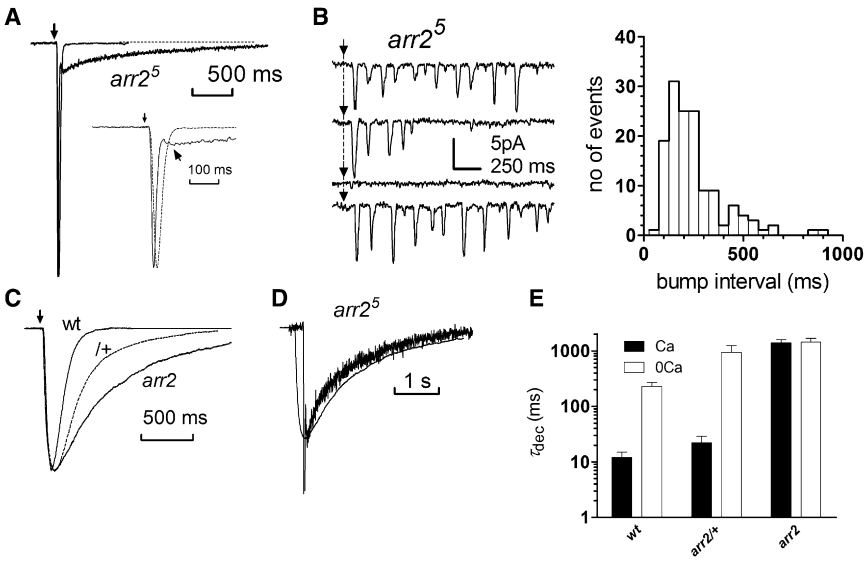

Figure 5. Responses in *arr2* Mutants

(A) Normalized flash response in wild-type and $arr2^5$ null mutant. Inset shows the response on a faster time base: note secondary peak (arrow) that decays slowly in $arr2^5$.

(B) Dim flashes containing only a single effective photon in $arr2^5$ elicited trains of quantum bumps (third flash was a "failure"); (right) bump interval distribution from such trains.

(C) Normalized, averaged flash responses in Ca^{2+}-free bath: $arr2^5$ decayed ~5-fold more slowly than in wild-type (wt); $arr2^5$/+ heterozygote (/+, dotted line) was intermediate.

(D) Responses from $arr2^5$ in the presence (noisy trace) and absence of Ca^{2+}; after normalizing and aligning the peaks of the responses (secondary peak in case of Ca^{2+} response), the deactivation time courses were nearly identical.

(E) Response decay time constants (τ_{dec} first-order exponentials fitted to tails of responses: mean ± SD, n = 4–13 cells per data point); note logarithmic scale.

Ca^{2+} Dependence of M* Inactivation Is Not Mediated via Phosphorylation of Rhodopsin

Drosophila Rh1 undergoes light-dependent phosphorylation and Ca^{2+}-dependent dephosphorylation (Bentrop and Paulsen, 1986; Steele et al., 1992; Byk et al., 1993; Lee and Montell, 2001; see Figure 8). Although most authors now suggest that M* phosphorylation is not required for Arr2 binding or response termination (e.g., Plangger et al., 1994; Vinos et al., 1997), Lee et al. (2004) recently suggested a role for rhodopsin kinase in regulating amplification, while the Ca^{2+}- and CaM-dependent rhodopsin phosphatase encoded by the *rdgC* gene has been proposed to play a role in response termination (Vinos et al., 1997; Lee and Montell, 2001).

Because of continuing uncertainty over the involvement of Rh1 (de)phosphorylation in response termination, we recorded from two transgenic Rh1 mutants lacking the C-terminal phosphorylation sites, as well as a mutant of rhodopsin phosphatase *rdgC*. All of these mutants had essentially wild-type responses, with no defects in deactivation or the Ca^{2+} dependence of M* deactivation (see Figure S3 and accompanying text). This strongly suggests that phosphorylation and dephosphorylation of rhodopsin play no direct role in M* inactivation or its Ca^{2+} dependence.

M* Inactivation Is Calmodulin Dependent, but Not Mediated by CamKII

Upon illumination, Arr2 is rapidly phosphorylated by CaMKII at a unique serine residue (Ser^{366}), and this has been suggested as a mechanism for Ca^{2+}-dependent M* inactivation (Matsumoto et al., 1994). This proposal was supported by finding that hypomorphic CaM mutants (*cam*) were defective in both CamKII function and M* inactivation (Scott et al., 1997). However, it was subsequently reported that Arr2 phosphorylation was not required for binding of Arr2 to M, but was required for Arr2 to dissociate from R *after* photoreisomerization from M (Alloway and Dolph, 1999) and also as a signal to prevent endocytotic internalization of R/M-Arr2 complexes (Kiselev et al., 2000; see Figure 8). According to these studies, any deactivation defects in mutants defective in Arr2 phosphorylation might thus be explained as an indirect consequence of the light-dependent sequestration of Arr2 by R/M.

To further test a possible role for Arr2 phosphorylation in M* inactivation, we recorded from two *arr2* mutants incapable of undergoing phosphorylation by CamKII: $Arr2^{S366A}$ (a transgenic fly with Ser^{366} substituted for alanine) and $arr2^1$ (a C-terminal truncation mutant lacking Ser^{366}) (Alloway and Dolph, 1999). Responses in $arr2^1$ appeared essentially wild-type in both Ca^{2+} and Ca^{2+}-free solutions, and although we found a minor deactivation defect in $Arr2^{S366A}$, response inactivation also remained strongly Ca^{2+} dependent (Figures 6A and 6C). The fact that responses in $Arr2^{S366A}$ were ~5-fold slower than in wild-type flies in both Ca^{2+} and Ca^{2+}-free solutions is likely to be a consequence of the low level of Arr2 protein (~20%) in these flies (Alloway and Dolph, 1999). We also recorded from a variety of transgenic lines with compromised CamKII function, including RNAi knockdown (Figure S4), but in all cases, response deactivation and its Ca^{2+} dependence were indistinguishable from wild-type controls. These results suggest that neither Arr2 phosphorylation nor CaMKII play any direct role in M* inactivation or its Ca^{2+} dependence.

Nevertheless, when we recorded from *cam* hypomorphs, we found that, as previously reported (Scott et al., 1997), light responses displayed a pronounced deactivation defect, which appeared to represent a failure in M* inactivation, since single photon absorptions produced long trains of quantum bumps, as is the case in *arr2* mutants (data not shown). However, in marked contrast to $Arr2^{S366A}$, response deactivation was never accelerated in the presence of Ca^{2+} (Figures 6B and 6C). We tested the hypothesis that the *cam* phenotype might be due to sequestration of Arr2 in R/M-Arr2 complexes by rearing *cam* flies on a VA– diet so that there should no longer be sufficient Rh1 to sequester a significant fraction of Arr2. However, despite an ~350 fold reduction in Rh1 level, there was no rescue of the deactivation phenotype (Figure 6C).

Another explanation for defective M* inactivation in *cam* mutants might be an altered subcellular distribution of Arr2—e.g.,

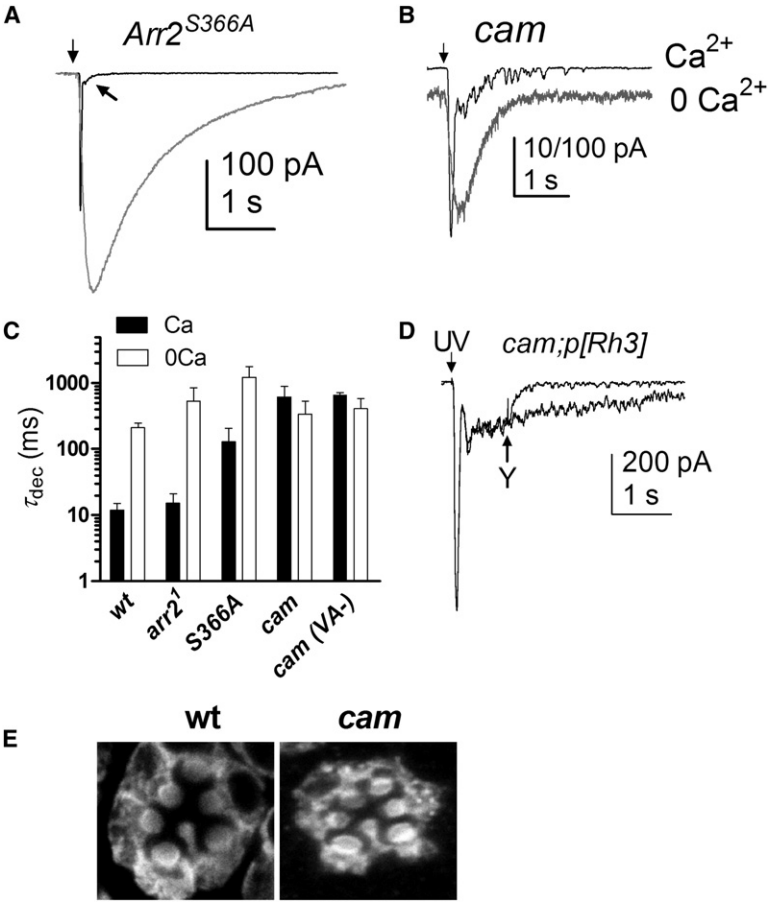

Figure 6. Responses in Arr2 Phosphorylation Mutant and *cam* Hypomorphs

(A) Flash responses in $Arr2^{S366A}$ showed a minor deactivation defect in the presence of Ca^{2+} (arrow), but under Ca^{2+}-free conditions response deactivation was ~10-fold slower (gray trace).

(B) By contrast, responses to brief flashes in cam^{339}/cam^{352} hypomorph (*cam*) decayed with a similar time course in Ca^{2+} and Ca^{2+}-free (gray trace) solutions.

(C) Single exponentials fitted to the decay (τ_{dec} mean ± SD, $Arr2^{S366A}$ n = 8, *cam* n = 11 cells); vitamin A deprivation (VA–, n = 3 cells) did not influence τ_{dec} in *cam* mutants.

(D) Photoreisomerization of M in *cam;p[Rh3]* flies by a Y flash rapidly terminated the response (cf. control response superimposed; n = 3).

(E) Immunolocalization of Arr2 in dark-adapted eyes from *cam* mutants (n = 7 flies) and wild-type control.

CaM might be required for Arr2 to enter the rhabdomeres. However, immunolocalization of Arr2 in *cam* hypomorphs closely resembled the wild-type pattern, with ~30% of the Arr2 in the rhabdomeres in the dark (Figure 6D). We also considered the possibility that the response deactivation defect in *cam* hypomorphs was not after all due to defective M* inactivation. To test this, we generated *cam* hypomorphs expressing Rh3 opsin (*cam;p[Rh3]*) and found that Y flashes delivered as long as 2 s after UV excitation completely suppressed the tail of the response (Figure 6E), clearly confirming that the deactivation defect represented a failure to inactivate M*.

Myosin III (NINAC) Is Required for Ca^{2+}-Dependent M* Inactivation

Our results indicate that CaM is required for Ca^{2+}-dependent inactivation of M* but that its effects are not mediated by CaMKII or RDGC. We therefore investigated another potential CaM-dependent target, the NINAC myosin III protein (Montell and Rubin, 1988). NINAC is a multifunctional protein with both myosin and kinase domains and is also reported to be the major CaM-binding protein in the photoreceptors (Porter et al., 1993). Null mutants of *ninaC* ($ninaC^{P235}$) are defective in several aspects of response deactivation, but despite extensive investigation (reviewed in Montell, 1999), the molecular basis has never been satisfactorily resolved, although an undefined role in M* inactivation has been suggested (Porter et al., 1995; Hofstee et al., 1996).

As previously reported (Hofstee et al., 1996), flashes delivered to $ninaC^{P235}$ photoreceptors evoked responses with a slowly deactivating tail, with a time constant of ~200 ms (Figure 7A). When flash intensities were reduced to the level of single photons, the deactivation defect was reflected in the generation of unequivocal multiple bump trains (Figure 7B, $p < 10^{-12}$, χ^2 test, n = 4, see Experimental Procedures), indicating a defect in M* inactivation. To confirm this interpretation, we generated $ninaC^{P235}$*;p[Rh3]* flies expressing Rh3 opsin and showed that the slowly decaying tail was rapidly suppressed by photoreconversion of M to R (Figure 7C).

Significantly, the deactivation time constant of flash responses recorded in $ninaC^{P235}$ in Ca^{2+}-free solutions (τ_{dec} 208 ± 76 ms, n = 8) was now indistinguishable from that measured from the same cells in the presence of Ca^{2+} (231 ± 92 ms), indicating that the Ca^{2+} dependence of M* inactivation was abolished (Figure 7E). Since microvillar CaM levels are reported to be greatly reduced in $ninaC^{P235}$ (Porter et al., 1993), this cannot distinguish between a direct involvement of the NINAC protein in Ca^{2+}-dependent inactivation or a requirement for CaM via some other pathway. However, the latter possibility was effectively excluded, since we also found a loss of Ca^{2+}-dependent M* inactivation in a *ninaC* transgenic mutant ($ninaC^{KD}$) with targeted deletion of the kinase domain (Porter and Montell, 1993), and which has normal levels of CaM in the microvilli (Figure 7F). As in $ninaC^{P235}$, the time constants of final response inactivation in the presence and absence of Ca^{2+} were indistinguishable, indicating that Ca^{2+} dependence of M* inactivation was effectively abolished (Figures 7D and 7E). Since CaM levels were normal in $ninaC^{KD}$, this suggests that functional NINAC protein itself is required to mediate rapid Ca-CaM-dependent M* inactivation and that its kinase domain is required for this function. However, kinase *activity* of NINAC appeared not to be required, as a point mutation in the presumptive ATP-binding

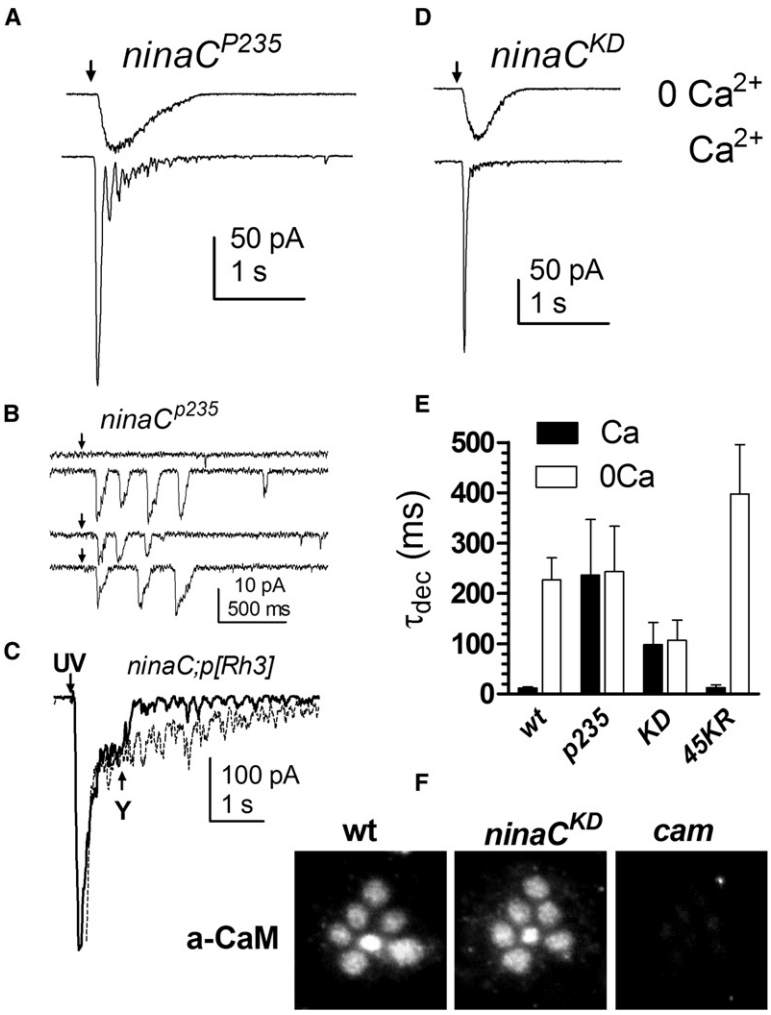

Figure 7. NINAC Is Required for Ca^{2+}-Dependent M* Inactivation

(A and B) Flash responses in both the null *ninaC*^{P235} mutant (A) and *ninaC*^{KD} lacking the kinase domain (B) showed a deactivation defect, with responses decaying with a similar time course in Ca^{2+} (top) and Ca^{2+}-free solutions (τ_{dec} plotted in [E]).

(C) Dim flashes containing only a single effective photon in *ninaC*^{P235} mutants elicited trains of quantum bumps (note "failure").

(D) Photoreisomerization of M* in *ninaC*^{P235}*;p[Rh3]* flies by a Y flash rapidly terminated the response to a UV flash (dotted line, control "UV only" response, n = 4).

(E) Deactivation time constants (τ_{dec}) from single exponentials fitted to the response decay in Ca^{2+} and Ca^{2+}-free solutions. In *ninaC*^{P235} and *ninaC*^{KD} mutants, τ_{dec} in Ca^{2+} and Ca^{2+}-free solutions was indistinguishable; however, responses in *ninaC*^{45KR} remained strongly Ca^{2+} dependent (mean ± SD, n = 6–14 cells—only 3 for 45KR).

(F) Immunolocalization of CaM in *ninaC*^{KD} (*n* = 5 flies) appeared similar to wild-type (n = 4), with strong labeling in the rhabdomeres. Greatly reduced labeling in *cam* hypomorph (n = 2) confirmed specificity of the antibody.

site (*ninaC*^{K45R}), expected to render the kinase inactive (Li et al., 1998), showed essentially wild-type behavior, with intact Ca^{2+}-dependent inactivation (Figure 7E). Interestingly, although *ninaC*^{KD} appeared to have lost Ca^{2+} dependence of M* inactivation, other electrophysiological aspects of the *ninaC* null phenotype, which include the occurrence of spontaneous bump-like events in the dark and an increased bump duration (Hofstee et al., 1996), were not reproduced. In other words, *ninaC*^{KD} appears to be specifically defective in Ca^{2+}-dependent M* inactivation, without the additional and potentially complicating phenotypes of the null mutation (*ninaC*^{P235}).

Strikingly, despite showing little or no Ca^{2+} dependence, response deactivation in *ninaC*^{KD} mutants under Ca^{2+}-free conditions was considerably faster (τ_{dec} ~100 ms) than in *ninaC*^{P235} or indeed than in wild-type flies (Figures 7D and 7E). Such an acceleration suggests that the Ca^{2+} dependence of M* inactivation might be achieved, at least in part, by a disinhibitory mechanism. Specifically, we hypothesize a mechanism whereby NINAC, or a NINAC-regulated target, binds Arr2 under low-Ca^{2+} conditions, thereby restricting its access to M*, and that Ca/CaM promotes the rapid release of Arr2. Such a model appears at odds with the lack of any such acceleration in the *ninaC*^{P235} null mutant, which has similar kinetics to wild-type flies under Ca^{2+}-free conditions. However, when we investigated the levels of Arr2 in *ninaC* mutants by western analysis (Table 1 and Figure S1), we found that Arr2 levels in both *ninaC*^{P235} (~50%) and *ninaC*^{KD} (~30%) were very significantly reduced compared to wild-type levels. We found an even greater reduction in Arr2 levels (~28% of wild-type levels) in *cam* hypomorphs. In otherwise wild-type flies, even a 50% reduction of Arr2 level (in *arr2*^{5}/+ heterozygotes) resulted in a deactivation time constant of ~1000 ms under Ca^{2+}-free conditions (Figures 5C and 5E), which is up to 10-fold slower than in any of these genetic backgrounds. Thus, in both *ninaC* and *cam* mutants, response deactivation under Ca^{2+}-free conditions was in fact profoundly accelerated compared to what would be expected on the basis of available arrestin.

DISCUSSION

We have exploited the bistable nature of invertebrate rhodopsins to measure the lifetime of activated metarhodopsin in *Drosophila*. Our approach, which measures the time window during which photoreisomerization of M* can suppress the response to light, was first used by Hamdorf and Kirschfeld (1980). Only one other study has used this strategy, namely Richard and Lisman (1992), who exploited the relative lack of overlap of the R and M spectra in UV opsins by recording from the UV-sensitive photoreceptors in *Limulus* median ocelli. We adapted this strategy for *Drosophila* by using flies engineered to express the UV opsin Rh3 and found that the effective M* lifetime was very short (τ_{dec} ≈ 20 ms) under physiological conditions. Strikingly, M* lifetime was prolonged ~10-fold in the absence of Ca^{2+} influx, indicating that M-Arr2 binding is Ca^{2+} dependent and that M* lifetime is the rate-limiting step in response deactivation in Ca^{2+}-free

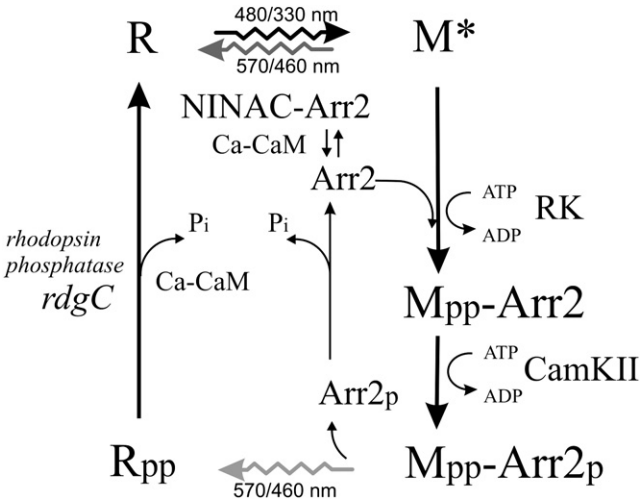

Figure 8. Rhodopsin Cycle and Role of NINAC in CaCaM-Dependent M* Inactivation

Photoisomerization of rhodopsin (R) by short-wavelength light (480 nm for Rh1 or 330 nm for Rh3) generates active metarhodopsin (M*). M* continues to activate G_q until it binds arrestin (Arr2) or is reconverted to R by long-wavelength illumination (570/460 nm). M is serially phosphorylated by rhodopsin kinase (RK), but this is not required for M* inactivation or Arr2 binding (Plangger et al., 1994; Vinos et al., 1997; Kiselev et al., 2000). CaMKII-dependent phosphorylation of Arr2 at Ser^{366} and photoreconversion of M_{pp} to R_{pp} is required for the release of Arr_p (Alloway and Dolph, 1999). Phosphorylation of Arr2 also prevents endocytotic internalization of M-Arr2 (Kiselev et al., 2000). In $Arr2^{S366A}$ or mutants defective in CamKII, photoreconversion fails to release Arr2. Finally, R_{pp} is dephosphorylated by the Ca-CaM-dependent rhodopsin phosphatase (*rdgC*) to recreate the ground state, R (Byk et al., 1993; Vinos et al., 1997; Lee and Montell, 2001). Our results suggest that under low-Ca^{2+} conditions Arr2 is prevented from rapid binding to M* because it is sequestered by NINAC or a NINAC-regulated target; however, Ca^{2+} influx acting via CaM rapidly releases Arr2. Each microvillus contains ~70 Arr2 molecules, ensuring rapid quenching of M* once they are free to diffuse. The role of M* phosphorylation remains uncertain but may be involved in Rh1 internalization by the minor arrestin, Arr1 (Satoh and Ready, 2005).

solutions. Further experiments led us to propose a mechanism for Ca^{2+}-dependent M* inactivation by Arr2, mediated by calmodulin (CaM) and myosin III NINAC (Figure 8).

Mechanism of Ca^{2+}-Dependent Arr2 Binding

Ca^{2+} dependence of M* lifetime had not previously been demonstrated in an invertebrate photoreceptor, and the consensus from data in *Drosophila* suggested no obvious mechanism by which M* lifetime could be regulated by Ca^{2+}. Our finding that M* inactivation was strongly Ca^{2+} dependent prompted us to re-examine possible roles of Rh1 and Arr2 phosphorylation as well as CaM. Although M* lifetime remained strongly Ca^{2+} dependent in mutants defective in rhodopsin and arrestin phosphorylation, the Ca^{2+} dependence of M* inactivation was effectively eliminated in hypomorphic *cam* mutants. This requirement for CaM appeared to be mediated by the myosin III NINAC protein, since the Ca^{2+} dependence of M* inactivation was effectively abolished in both the null $ninaC^{P235}$ mutant and an allele ($ninaC^{KD}$) in which CaM levels in the microvilli were unaffected. NINAC, which is the major CaM-binding protein in the photoreceptors, has long been known to be required for normal rapid response deactivation (Porter et al., 1992), but the mechanistic basis remained unresolved. Our results now strongly suggest that it is specifically required for the Ca^{2+}- and CaM-dependent inactivation of M* by Arr2.

How might NINAC regulate the Ca^{2+}-dependent inactivation of M*? A clue comes from the finding that Arr2 levels were substantially reduced in *ninaC* mutants. After taking this into account, the lack of Ca^{2+} dependence of M* inactivation in *ninaC* mutants was in fact associated with a very pronounced *acceleration* of response inactivation under Ca^{2+}-free conditions. This was most clearly revealed in $ninaC^{KD}$, which appears to be specifically defective only in Ca^{2+}-dependent M* inactivation and does not show the additional response defects of the null *ninaC* phenotype (e.g., Hofstee et al., 1996). This suggests a disinhibitory mechanism whereby Ca^{2+}-dependent inactivation of M* may be achieved, at least in part, by the NINAC-dependent prevention of Arr2-M* binding under low-Ca^{2+} conditions. Specifically, we suggest that in Ca^{2+}-free solutions, or in the low-Ca^{2+} conditions prevailing during the latent period of the quantum bump under physiological conditions, Arr2 in the microvilli is predominantly bound to NINAC or a NINAC-regulated target, thus restricting its access to M*. However, following Ca^{2+} influx, CaCaM would bind to NINAC, causing NINAC to release Arr2, which, as a soluble protein, could then rapidly diffuse to encounter and inactivate M* (Figure 8).

Interestingly, a recent study reported that NINAC can interact with Arr2 in a phosphoinositide-dependent manner (Lee and Montell, 2004). This interaction was described in the context of a role of NINAC in light-induced translocation of Arr2, which was reported to be disrupted in *ninaC* mutants. However, involvement in translocation was challenged by a subsequent study reporting that Arr2 translocation was unaffected in *ninaC* mutants (Satoh and Ready, 2005). It will be interesting to see whether the Arr2-NINAC interactions described by Lee and Montell (2004) reflect a role in the CaCaM- and NINAC-dependent inactivation of M* reported here.

Functional Implications

M-Arr2 Binding Is Only Rate Limiting under Ca^{2+}-Free Conditions

It has long been known that responses under Ca^{2+}-free conditions decay ~10-fold more slowly than in the presence of Ca^{2+} (Hardie, 1991; Ranganathan et al., 1991). Our results now establish that the inactivation of M* by Arr2 is the rate-limiting inactivation step in such Ca^{2+}-free responses, with a time constant of ~200 ms in wild-type photoreceptors. Following inactivation of M* by photoreisomerization under Ca^{2+}-free conditions, the response decayed with a time constant of ~80 ms. This also provides a unique and direct measure of the time constant(s) of the downstream mechanisms of inactivation, which presumably include GTP-ase activity of the Gq-PLC complex (Cook et al., 2000) and removal of DAG by DAG kinase (Raghu et al., 2000). It will be interesting so see whether Ca^{2+} also accelerates these inactivation mechanisms.

By contrast, the failure to accelerate response decay by overexpressing Arr2 in the presence of Ca^{2+} (Figure 4) indicates that

Table 2. Mutants Used

Allele	Description	Protein Level (%WT)	Reference
$arr2^5$	null Arr2 mutant: stop codon at Tyr^{20}	0%	Alloway and Dolph, 1999
$arr2^1$	truncated at P^{261}	80%	Dolph et al., 1993
$p[Arr2^{S366A}];arr2^5$; abbreviated to $Arr2^{S366A}$	genomic Arr2 transgene with Ser^{366} mutated to alanine on $arr2^5$ null background	21%	Alloway and Dolph, 1999
p[Arr2]	genomic wild-type Arr2 transgene on wild-type background	193%	Ranganathan and Stevens, 1995
e^s , $ninaE^{EI17}$, p_{ninaE}[Rh3]; abbreviated to *p[Rh3]*	UV opsin, Rh3 under *ninaE* promoter; on *ninaE* null background	50%	Feiler et al., 1992
e^s ,$ninaE^{Ei17}$,p_{ninaE} $[Rh1^{\Delta 356}]$; abbr. to $Rh1^{\Delta 356}$	Rh1 transgene, truncated at 356	~50%	Vinos et al., 1997
e^s ,$ninaE^{Ei17}$,p_{ninaE} $[Rh1^{C\ TS>A}]$; abbr. to $Rh1^{CTSA}$	Rh1 transgene: 3 C-terminal serines mutated to alanine	~75%	Kiselev et al., 2000
$rdgC^{306}$	null allele of rhodopsin phosphatase	0%	Steele et al., 1992
$yw;cam^{352}/cam^{339}$; abbr. to *cam*	heteroallelic: cam^{339} null over cam^{352} hypomorph	~10%	Scott et al., 1997
$ninaC^{P235}$	null mutant of NINAC (myosin III)	0%	Matsumoto et al., 1987; Montell and Rubin, 1988
$ninaC^{P235}$;$p[ninaC^{KD}]$; abbr. to $ninaC^{KD}$	NINAC transgene lacking kinase domain (aa 17–284) on $ninaC^{P235}$ null background	>50%	Porter and Montell, 1993
$ninaC^{P235}$;$p[ninaC^{45KR}]$; abbr. to $ninaC^{45KR}$	point mutation in ATP-binding site of kinase domain on $ninaC^{P235}$ null background	>50%	Li et al., 1998

inactivation of M* is *not* rate limiting under physiological conditions. This can be understood by recognizing that the macroscopic kinetics are determined by the convolution of the bump latency distribution and bump waveform (Henderson et al., 2000), the latter probably terminated by Ca^{2+}-dependent inactivation of the light-sensitive channels. Until the Ca^{2+} influx associated with the quantum bump, the phototransduction machinery in each microvillus is effectively operating under Ca^{2+}-free conditions. Our results suggest that it is the Ca^{2+} influx associated with each quantum bump that promotes M* inactivation, and hence the timing of M* inactivation will be determined by the bump latency distribution and not vice versa. This leads to the, perhaps counterintuitive, concept that response termination is rate limited, not by any specific inactivation mechanism, but rather by the time course with which the cumulative probability of bump generation approaches 100%.

Ca^{2+}-Dependent M* Inactivation Promotes Sensitivity, Fidelity, and Temporal Resolution of Phototransduction

Clearly, rapid quenching of M* is essential to maintain the fidelity and high temporal resolution of phototransduction. In wild-type cells, an effectively absorbed photon generates only one quantum bump, but never (or extremely rarely) two or more; yet the multiple bump trains observed in *arr2*, *cam*, and *ninaC* mutants show that additional bumps are readily generated within 50–100 ms if M* fails to be inactivated (e.g., Figure 5B). To prevent such multiple bumps without Ca^{2+}-dependent feedback would require such a high rate of Arr2 binding that many M* molecules would be inactivated before they had a chance to activate sufficient G proteins to generate a quantum bump. This would result in an effective reduction in sensitivity, as is directly illustrated by the phenotype of *p[Arr2]* flies overexpressing Arr2 (Figure 4). These show not only a 5-fold reduction in Q.E. but also a reduction in bump amplitude and even an increase in bump latency, which we attribute to a decreased rate of second messenger generation. The mechanism we propose here provides an elegant solution to this dilemma. Our analysis suggests that in the low-Ca^{2+} environment prior to Ca^{2+} influx, much of the Arr2 in the microvillus is bound to NINAC (or NINAC-regulated target), thus allowing M* to remain active long enough to activate sufficient G proteins to guarantee production of a full-sized quantum bump with high probability. Only after the bump has been initiated does Ca^{2+} influx accelerate the inactivation of M* by releasing Arr2, thus ensuring that only one bump is generated. This strategy is complemented and enabled by the ultracompartmentalization afforded by the microvillar design, which ensures that the Ca^{2+} rise is both extremely rapid and largely confined to the affected microvillus.

EXPERIMENTAL PROCEDURES

Flies

Drosophila melanogaster were raised in the dark at 25°C. The wild-type strain was Oregon w^{1118}; the mutant and transgenic lines used are summarized in Table 2. Various genetic combinations (see Results) were generated by standard crosses using appropriate balancers.

For Vitamin A deprivation, flies were raised on a diet consisting of agar, yeast, sucrose, and cholesterol (Isono et al., 1988). The reduction in rhodopsin levels was estimated by counting quantum bumps in response to calibrated stimuli, indicating an ~350-fold reduction compared to flies reared on the normal control diet (based on agar, cornmeal, glucose, and yeast).

Whole-Cell Recordings

Dissociated ommatidia from newly eclosed adult flies were prepared as previously described (Hardie, 1991; Hardie et al., 2001) and transferred to a recording chamber on an inverted microscope at room temperature (20°C ± 1°C). The

standard bath contained (in mM) 120 NaCl, 5 KCl, 10 *N*-Tris-(hydroxymethyl)-methyl-2-amino-ethanesulphonic acid (TES), 4 $MgCl_2$, 1.5 $CaCl_2$, 25 proline, and 5 alanine. The Ca^{2+}-free bath was identical except for the omission of $CaCl_2$ and the addition of 2 mM Na_4EGTA. The Ca^{2+}-free solution was applied by broad-mouthed (~10 μm) puffer pipettes (Hardie and Mojet, 1995). The intracellular solution was (in mM) 140 Kgluconate, 10 TES, 4 MgATP, 2 $MgCl_2$, 1 NAD, and 0.4 NaGTP. The pH of all solutions was adjusted to 7.15. All chemicals were obtained from Sigma-Aldrich. Whole-cell voltage-clamp recordings were made at −70 mV (including correction for −10 mV junction potential) using electrodes of resistance ~10–15 MΩ. Series resistance values were generally below 30 MΩ and routinely compensated to >80% for currents greater than 100 pA. Data were collected and analyzed using Axopatch 200 or 1-D amplifiers and pCLAMP 9 software (Molecular Devices, Union City CA). Quantum bumps were analyzed using "Minianalysis" (Jaejin Software Leonia, NJ).

Light Stimulation

Photoreceptors were stimulated via a green LED, with maximum intensity of 3×10^8 effectively absorbed photons s^{-1} per photoreceptor, or, for cells expressing Rh3, a UV LED (Maplins UK, λ_{max} 380 nm; maximum intensity of ~5×10^5 effectively absorbed photons s^{-1}). Unless otherwise stated, photoreceptors were stimulated with brief (1 ms) flashes containing less than 500 effectively absorbed photons, generating responses in the strictly linear range. Intensities were calibrated by counting quantum bumps at low intensities (e.g., Henderson et al., 2000). To test whether single photons elicited single or multiple quantum bumps, 100 or more brief (≤1 ms) flashes containing on average less than one effective photon were delivered, and the mean quantal content (m) of the flash was calculated from the fraction (P_0) of flashes that induced no quantum bumps (failures), according to the Poisson distribution:

$$m = -\ln(P_0) \quad (1)$$

the probability (P_n) of flashes containing 1, 2, 3,…n effective photons is given by:

$$P_n = e^{-m} \times m^n/n! \quad (2)$$

Wild-type photoreceptors conformed closely to the Poisson prediction (p typically > 0.9 using the χ^2 statistic).

Quantitative photoreisomerization of Rh3 M* was achieved using a brief (~1 ms) flash from a Hi-Tech Xenon arc XF10 flash unit (Rapp OptoElectronic, Hamburg Germany) delivered antidromically via the fluorescence port of the microscope and filtered by a Schott GG495 filter. The ability of this stimulus to hit essentially every metarhodopsin molecule in the cell was demonstrated by the almost complete suppression of the response to the UV test flash when delivered within 2–5 ms of the UV test (e.g., Figure 2).

Immunolocalization and Western Blots

Indirect immunohistochemistry was carried out as previously described using confocal microscopy of whole-mounted retinae (Satoh and Ready, 2005). Eyes were dissected from young flies (0–2 days unless otherwise stated) and fixed using infrared illumination and infrared-sensitive eyepieces. Primary antisera were rabbit anti- Arr2 (gift from Dr. R. Ranganathan) and rabbit anti-Cam (gift from Dr. C. Klee); secondary antibody was anti-rabbit labeled with Cy2 (1:300) (Amersham-Pharmica).

For western blots, 1-day-old fly heads were homogenized in RIPA buffer (150 mM NaCl, 50 mM Tris-HCl [pH 8.2], 1% Triton, 0.5% sodium deoxycholate, and 0.1% SDS) with a Pellet Pestle (Kimble-Kontes, Vineland, NJ). The sample proteins (diluted with SDS loading buffer to make 0.05 fly head per lane) were fractionated by SDS-PAGE and transferred to Amersham Hybond-P transfer membranes (GE Healthcare) in Tris-glycine buffer. The blots were probed with primary rabbit antibodies: either 1/1000 dilution anti-α-tubulin (Abcam, ab15246) or 1/1000 dilution anti-Arr2 and then subsequently with 1/3000 dilution anti-rabbit IgG peroxidase conjugate (Promega, w401B). The signals were detected using ECL reagents (GE Healthcare).

SUPPLEMENTAL DATA

The Supplemental Data include four figures and can be found with this article online at http://www.neuron.org/cgi/content/full/59/5/778/DC1/.

ACKNOWLEDGMENTS

This research was supported by the Biotechnology and Biological Sciences Research Council (BB/D D00785/1, E19850: R.C.H., C.-H.L., M.P., J.H.) and the NIH (NEI10306: D.F.R., A.K.S.). Gifts of mutant, transgenic flies, and/or reagents from Drs K. Beckingham, P. Dolph, L. Griffith, C. Montell, W.L. Pak, J. O'Tousa, and C.S. Zuker are gratefully acknowledged.

Accepted: July 9, 2008
Published: September 10, 2008

REFERENCES

Alloway, P.G., and Dolph, P.J. (1999). A role for the light-dependent phosphorylation of visual arrestin. Proc. Natl. Acad. Sci. USA *96*, 6072–6077.

Bentrop, J., and Paulsen, R. (1986). Light-modulated ADP-ribosylation, protein phosphorylation and protein binding in isolated fly photoreceptor membranes. Eur. J. Biochem. *161*, 61–67.

Byk, T., BarYaacov, M., Doza, Y.N., Minke, B., and Selinger, Z. (1993). Regulatory arrestin cycle secures the fidelity and maintenance of the fly photoreceptor cell. Proc. Natl. Acad. Sci. USA *90*, 1907–1911.

Cook, B., BarYaacov, M., BenAmi, H.C., Goldstein, R.E., Paroush, Z., Selinger, Z., and Minke, B. (2000). Phospholipase C and termination of G-protein-mediated signalling in vivo. Nat. Cell Biol. *2*, 296–301.

Dolph, P.J., Ranganathan, R., Colley, N.J., Hardy, R.W., Socolich, M., and Zuker, C.S. (1993). Arrestin function in inactivation of G protein-coupled receptor rhodopsin in vivo. Science *260*, 1910–1916.

Feiler, R., Bjornson, R., Kirschfeld, K., Mismer, D., Rubin, G.M., Smith, D.P., Socolich, M., and Zuker, C.S. (1992). Ectopic expression of ultraviolet-rhodopsins in the blue photoreceptor cells of *Drosophila*: visual physiology and photochemistry of transgenic animals. J. Neurosci. *12*, 3862–3868.

Govardovskii, V.I., Fyhrquist, N., Reuter, T., Kuzmin, D.G., and Donner, K. (2000). In search of the visual pigment template. Vis. Neurosci. *17*, 509–528.

Gu, Y., Oberwinkler, J., Postma, M., and Hardie, R.C. (2005). Mechanisms of light adaptation in *Drosophila* photoreceptors. Curr. Biol. *15*, 1228–1234.

Hamdorf, K., and Kirschfeld, K. (1980). Reversible events in the transduction process of photoreceptors. Nature *283*, 859–860.

Hardie, R.C. (1991). Whole-cell recordings of the light-induced current in *Drosophila* photoreceptors: evidence for feedback by calcium permeating the light sensitive channels. Proc. R. Soc. Lond. B. Biol. Sci. *245*, 203–210.

Hardie, R.C. (1995). Photolysis of caged Ca^{2+} facilitates and inactivates but does not directly excite light-sensitive channels in *Drosophila* photoreceptors. J. Neurosci. *15*, 889–902.

Hardie, R.C. (2007). TRP channels and lipids: from Drosophila to mammalian physiology. J. Physiol. *578*, 9–25.

Hardie, R.C., and Minke, B. (1992). The *trp* gene is essential for a light-activated Ca^{2+} channel in Drosophila photoreceptors. Neuron *8*, 643–651.

Hardie, R.C., and Mojet, M.H. (1995). Magnesium-dependent block of the light-activated and *trp*-dependent conductance in *Drosophila* photoreceptors. J. Neurophysiol. *74*, 2590–2599.

Hardie, R.C., and Raghu, P. (2001). Visual transduction in *Drosophila*. Nature *413*, 186–193.

Hardie, R.C., and Postma, M. (2008). Phototransduction in microvillar photoreceptors of Drosophila and other invertebrates. In The Senses: A Comprehensive Reference, *Volume 1, Vision 1*, A.I. Basbaum, A. Kaneko, G.M. Shepherd, and G. Westheimer, eds. (San Diego, CA: Academic Press), pp. 77–130.

Hardie, R.C., Raghu, P., Moore, S., Juusola, M., Baines, R.A., and Sweeney, S.T. (2001). Calcium influx via TRP channels is required to maintain PIP_2 levels in *Drosophila* photoreceptors. Neuron *30*, 149–159.

Hardie, R.C., Martin, F., Cochrane, G.W., Juusola, M., Georgiev, P., and Raghu, P. (2002). Molecular basis of amplification in *Drosophila*

phototransduction. Roles for G protein, phospholipase C, and diacylglycerol kinase. Neuron *36*, 689–701.

Henderson, S.R., Reuss, H., and Hardie, R.C. (2000). Single photon responses in *Drosophila* photoreceptors and their regulation by Ca^{2+}. J. Physiol. *524*, 179–194.

Hillman, P., Hochstein, S., and Minke, B. (1983). Transduction in invertebrate photoreceptors: role of pigment bistability. Physiol. Rev. *63*, 668–772.

Hofstee, C.A., Henderson, S., Hardie, R.C., and Stavenga, D.G. (1996). Differential effects of NINACproteins (p132 and p174) on light-activated currents and pupil mechanism in *Drosophila* photoreceptors. Vis. Neurosci. *13*, 897–906.

Isono, K., Tanimura, T., Oda, Y., and Tsukahara, Y. (1988). Dependency on light and vitamin A derivatives of the biogenesis of 3- hydroxyretinal and visual pigment in the compound eyes of Drosophila melanogaster. J. Gen. Physiol. *92*, 587–600.

Kawamura, S. (1993). Rhodopsin phosphorylation as a mechanism of cyclic GMP phosphodiesterase regulation by S-modulin. Nature *362*, 855–857.

Kiselev, A., Socolich, M., Vinos, J., Hardy, R.W., Zuker, C.S., and Ranganathan, R. (2000). A molecular pathway for light-dependent photoreceptor apoptosis in Drosophila. Neuron *28*, 139–152.

Lee, S.J., and Montell, C. (2001). Regulation of the rhodopsin protein phosphatase, RDGC, through interaction with calmodulin. Neuron *32*, 1097–1106.

Lee, S.J., and Montell, C. (2004). Light-dependent translocation of visual arrestin regulated by the NINAC myosin III. Neuron *43*, 95–103.

Lee, S.J., Xu, H., Kang, L.W., Amzel, L.M., and Montell, C. (2003). Light adaptation through phosphoinositide-regulated translocation of Drosophila visual arrestin. Neuron *39*, 121–132.

Lee, S.-J., Xu, H., and Montell, C. (2004). Rhodopsin kinase activity modulates the amplitude of the visual response in Drosophila. Proc. Natl. Acad. Sci. USA *101*, 11874–11879.

Li, H.S., Porter, J.A., and Montell, C. (1998). Requirement for the NINAC kinase/myosin for stable termination of the visual cascade. J. Neurosci. *18*, 9601–9606.

Matsumoto, H., Isono, K., Pye, Q., and Pak, W.L. (1987). Gene encoding cytoskeletal proteins in Drosophila rhabdomeres. Proc. Natl. Acad. Sci. USA *84*, 985–989.

Matsumoto, H., Kurien, B.T., Takagi, Y., Kahn, E.S., Kinumi, T., Komori, N., Yamada, T., Hayashi, F., Isono, K., Pak, W.L., et al. (1994). Phosrestin I undergoes the earliest light-induced phosphorylation by a calcium/calmodulin-dependent protein kinase in Drosophila photoreceptors. Neuron *12*, 997–1010.

Minke, B., and Parnas, M. (2006). Insights on TRP channels from in vivo studies in *Drosophila*. Annu. Rev. Physiol. *68*, 649–684.

Mishra, P., Socolich, M., Wall, M.A., Graves, J., Wang, Z., and Ranganathan, R. (2007). Dynamic scaffolding in a G protein-coupled signaling system. Cell *131*, 80–92.

Montell, C. (1999). Visual transduction in *Drosophila*. Annu. Rev. Cell Dev. Biol. *15*, 231–268.

Montell, C., and Rubin, G.M. (1988). The Drosophila ninaC locus encodes two photoreceptor cell specific proteins with domains homologous to protein kinases and the myosin heavy chain head. Cell *52*, 757–772.

Montell, C., and Rubin, G.M. (1989). Molecular characterization of Drosophila *trp* locus, a putative integral membrane protein required for phototransduction. Neuron *2*, 1313–1323.

Oberwinkler, J., and Stavenga, D.G. (2000). Calcium transients in the rhabdomeres of dark- and light-adapted fly photoreceptor cells. J. Neurosci. *20*, 1701–1709.

Plangger, A., Malicki, D., Whitney, M., and Paulsen, R. (1994). Mechanism of arrestin 2 function in rhabdomeric photoreceptors. J. Biol. Chem. *269*, 26969–26975.

Porter, J.A., and Montell, C. (1993). Distinct roles of the Drosophila *ninaC* kinase and myosin domains revealed by systematic mutagenesis. J. Cell Biol. *122*, 601–612.

Porter, J.A., Hicks, J.L., Williams, D.S., and Montell, C. (1992). Differential localizations of and requirements for the two *Drosophila ninaC* kinase/myosins in photoreceptor cells. J. Cell Biol. *116*, 683–693.

Porter, J.A., Yu, M., Doberstein, S.K., Pollard, T.D., and Montell, C. (1993). Dependence of calmodulin localization in the retina on the NINAC unconventional myosin. Science *262*, 1038–1042.

Porter, J.A., Minke, B., and Montell, C. (1995). Calmodulin binding to *Drosophila* NinaC required for termination of phototransduction. EMBO J. *14*, 4450–4459.

Postma, M., Oberwinkler, J., and Stavenga, D.G. (1999). Does Ca^{2+} reach millimolar concentrations after single photon absorption in *Drosophila* photoreceptor microvilli? Biophys. J. *77*, 1811–1823.

Raghu, P., Usher, K., Jonas, S., Chyb, S., Polyanovsky, A., and Hardie, R.C. (2000). Constitutive activity of the light-sensitive channels TRP and TRPL in the Drosophila diacylglycerol kinase mutant, *rdgA*. Neuron *26*, 169–179.

Ranganathan, R., and Stevens, C.F. (1995). Arrestin binding determines the rate of inactivation of the G protein-coupled receptor rhodopsin in vivo. Cell *81*, 841–848.

Ranganathan, R., Harris, G.L., Stevens, C.F., and Zuker, C.S. (1991). A *Drosophila* mutant defective in extracellular calcium-dependent photoreceptor deactivation and rapid desensitization. Nature *354*, 230–232.

Ranganathan, R., Bacskai, B.J., Tsien, R.Y., and Zuker, C.S. (1994). Cytosolic calcium transients: Spatial localization and role in Drosophila photoreceptor cell function. Neuron *13*, 837–848.

Richard, E.A., and Lisman, J.E. (1992). Rhodopsin inactivation is a modulated process in Limulus photoreceptors. Nature *356*, 336–338.

Satoh, A.K., and Ready, D.F. (2005). Arrestin1 mediates light-dependent rhodopsin endocytosis and cell survival. Curr. Biol. *15*, 1722–1733.

Scott, K., Becker, A., Sun, Y., Hardy, R., and Zuker, C. (1995). $G_q\alpha$ protein function in vivo: Genetic dissection of its role in photoreceptor cell physiology. Neuron *15*, 919–927.

Scott, K., Sun, Y.M., Beckingham, K., and Zuker, C.S. (1997). Calmodulin regulation of Drosophila light-activated channels and receptor function mediates termination of the light response in vivo. Cell *91*, 375–383.

Smith, D.P., Ranganathan, R., Hardy, R.W., Marx, J., Tsuchida, T., and Zuker, C.S. (1991). Photoreceptor deactivation and retinal degeneration mediated by a photoreceptor-specific protein-kinase-C. Science *254*, 1478–1484.

Stavenga, D.G. (1996). Insect retinal pigments: Spectral characteristics and physiological functions. Prog. Retin. Eye Res. *15*, 231–259.

Steele, F.R., Washburn, T., Rieger, R., and O'Tousa, J.E. (1992). Drosophila retinal degeneration C (*rdgC*) encodes a novel serine/threonine protein phosphatase. Cell *69*, 669–676.

Vinos, J., Jalink, K., Hardy, R.W., Britt, S.G., and Zuker, C.S. (1997). A G protein-coupled receptor phosphatase required for rhodopsin function. Science *277*, 687–690.

Wang, T., and Montell, C. (2007). Phototransduction and retinal degeneration in *Drosophila*. Pflugers Arch. *454*, 821–847.